Enhanced Monolithic Bidirectional Dual-Gate GaN HEMT Switch with Split Source Field Plates for Current Collapse Suppression

Yu-Ting Huang[1], Xiao-Quan Wu[1], Sheng-Hsi Hung[1], Tz-Wun Wang[1], Chi-Yu Chen[1], Po-Jui Chiu[1], Chien-Wei Cho[1], Tay Jye Ni[1], Ke-Horng Chen[1], Ying-Hsi Lin[2], Tsung-Yen Tsai[2], Shian-Ru Lin[2], Hann-Huei Tsai[3]
[1]National Yang Ming Chiao Tung University, Taiwan, [2]Realtek Semiconductor, Taiwan, [3]Taiwan Semiconductor Research Institute, Taiwan

***Abstract*—This paper presents a Monolithic Bidirectional Dual-Gate (MBD) Gallium Nitride (GaN) High Electron Mobility Transistor (HEMT) switch enhanced with Split Source Field Plates (SSFPs). The monolithic architecture reduces both device area and on-resistance (R_{ON}) compared to conventional discrete topologies. The inclusion of SSFPs effectively moderates electric field concentration, mitigates current collapse, and preserves low R_{ON} under high-voltage off-state stress. Experimental results show that the proposed switch limits R_{ON} degradation to just 42% after repeated current collapse events. Additionally, the device area is reduced by 31% relative to back-to-back discrete GaN HEMTs. These advancements improve both efficiency and integration, positioning the proposed switch as a compelling solution for next-generation bidirectional power applications.**

Keywords*—bidirectional switch, current collapse, field plate, GaN HEMT

I. Introduction

With the rapid rise of bidirectional converters, a robust infrastructure is crucial to support multifunctional energy distribution—driving the need for efficient bidirectional power switches [1]–[6]. As shown in Fig. 1(a), these switches play a critical role in bidirectional battery chargers, allowing seamless two-way energy flow while blocking reverse current. Fig. 1(b) outlines the characteristics and limitations of existing bidirectional switch architectures. Diode-integrated insulated-gate bipolar transistor (IGBT) switches [1] suffer from a built-in diode threshold voltage, which increases conduction losses and reduces overall efficiency. On the other hand, discrete back-to-back (B2B) topologies [2]–[4] eliminate threshold voltage concerns but at the cost of doubling the on-resistance (R_{ON}) in the current path, leading to higher conduction losses and increased die area.

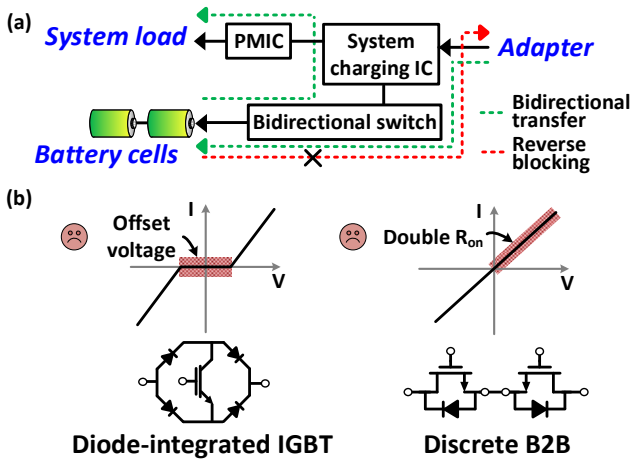

Fig. 1. (a) The battery charger requires a bidirectional switch to facilitate energy transfer and block reverse current. (b) Characteristics and limitations of current bidirectional switches.

To overcome the limitations of conventional designs, monolithic bidirectional dual-gate (MBD) Gallium Nitride (GaN) High Electron Mobility Transistor (HEMT) switches have been introduced [5]–[6]. Leveraging GaN's inherently low R_{ON} and the compactness of monolithic integration, these switches achieve reduced on-resistance and minimized die area, as illustrated in Fig. 2. In the off-state, both gate voltages (V_{G1S1} and V_{G2S2}) are set to 0 V, fully disabling the switch. Even if either source terminal (S_1 or S_2) is exposed to a higher voltage, reverse current is effectively blocked—unlike in conventional single MOSFETs, which suffer from body diode conduction and reverse leakage. In the on-state, applying 6 V to both gates enables bidirectional current flow with ultra-low R_{ON}. The switch can also operate in a diode mode, where current is allowed in one direction by setting one gate to 6 V and the other to 0 V. This flexible control capability ensures efficient and reliable operation in bidirectional power applications.

II. Proposed Split Source Field Plate Structure

However, despite the ultra-low R_{ON} advantage of bidirectional GaN-based switches, GaN HEMTs are prone to current collapse due to charge trapping effects caused by lattice defects, impurities, and other structural imperfections [7]. Under off-state stress, the high electric field between the gate and drain leads to electron trapping in the gate insulator. These trapped charges gradually deplete the two-dimensional electron gas (2DEG) channel, hindering current flow and increasing R_{ON}. This issue is further intensified in monolithic bidirectional dual-gate (MBD) GaN HEMT switches, where electron trapping can occur on both gate sides, effectively doubling the severity of the current collapse. As illustrated in Fig. 3, this leads to a more pronounced increase in R_{ON} over time.

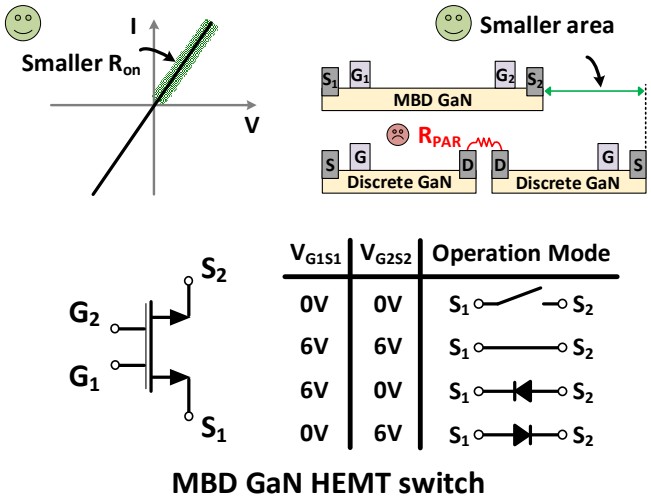

Fig. 2. The advantages of the monolithic bidirectional dual-gate GaN HEMT switch and its working principle.

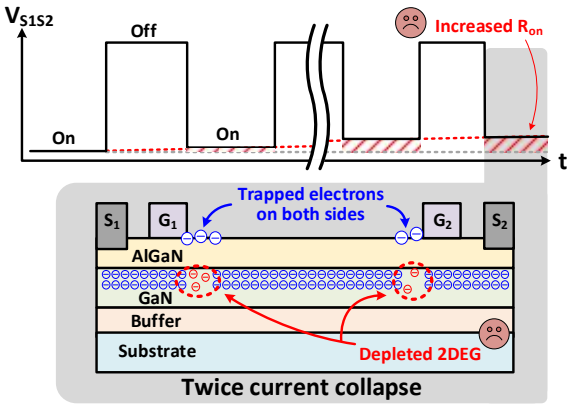

Fig. 3. Mechanism of twice current collapse on the monolithic bidirectional dual-gate GaN HEMT switch.

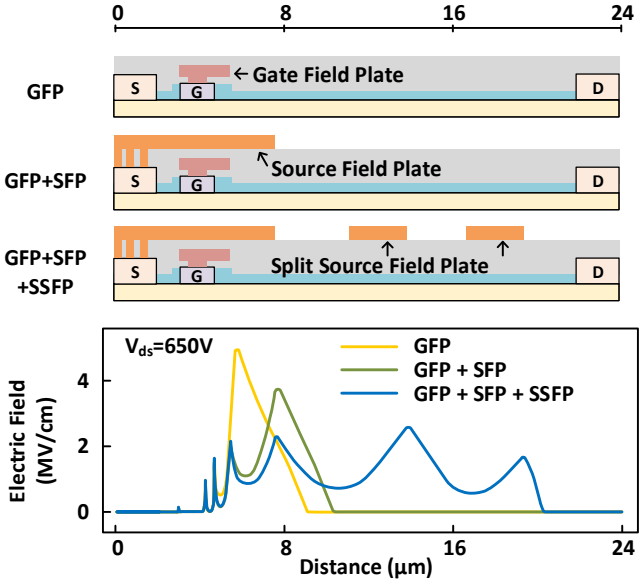

Fig. 4. The cross-section of GaN HEMTs with different field plate designs and the corresponding electric field distributions.

Integrating a source field plate (SFP) into GaN HEMTs has been shown to effectively suppress the peak electric field, thereby alleviating current collapse issues [8]–[9]. Fig. 4 illustrates cross-sectional views of GaN HEMTs featuring various field plate configurations, along with their corresponding electric field distributions. From top to bottom, the configurations include a gate field plate (GFP), a GFP combined with a conventional SFP, and the proposed split source field plate (SSFP). The introduction of the SSFP further reduces peak electric field intensity and promotes a more uniform field distribution along the edges of the SFP and SSFP. This enhancement significantly mitigates electron trapping, reducing the severity of current collapse and improving device reliability.

III. Proposed Monolithic Bidirectional GaN HENT Switch with Split Source Field Plates

To address the dual current collapse issue inherent in monolithic bidirectional (MBD) GaN HEMT switches, which significantly impacts efficiency, a novel SSFP-based MBD GaN HEMT switch is proposed. Fig. 5 presents the architecture of the switch, highlighting the integration of split source field plates (SSFPs), along with cross-sectional views captured by a scanning electron microscope (SEM). The device is fabricated on a 6-inch GaN-on-Si wafer, consisting of a low-resistivity silicon substrate, a GaN buffer/transition layer, and a p-GaN gate layer. The SFPs and SSFPs are implemented using Aluminum-Copper (AlCu) interconnects approximately 1.5 μm thick, enabling robust current handling. The gate field plate (GFP) is formed using a Schottky contact metal with a thickness roughly one-fifth that of the SFP, interfacing directly with the p-GaN layer and incorporating Nickel Silicide (NiSi) to improve electrical performance and reliability.

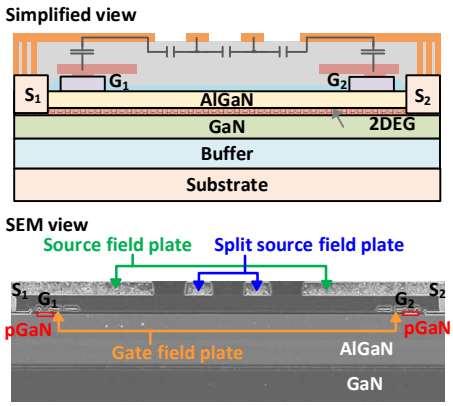

Fig. 5. The SEM image of the cross-sectional view of the proposed MBD GaN HEMT switch.

IV. Device Performance

A. Static I-V characteristics

Fig. 6 illustrates the static I-V characteristics of the GFP-based MBD switch across three operating modes: (a) bidirectional conduction, (b) single-ended conduction in diode mode, and (c) off-state with no conduction. Similarly, Figs. 7 and 8 present the corresponding characteristics for the SFP-based and SSFP-based MBD switches, respectively. The GFP MBD switch exhibits an R_{ON} of 19.88 Ω·mm at V_{GS} = 6 V, while the SFP version achieves a reduced R_{ON} of 18.92 Ω·mm. The SSFP MBD switch follows closely with an R_{ON} of 19.28 Ω·mm. All three designs demonstrate robust reverse-blocking capability and a consistent diode-mode offset voltage of approximately 1.65 V. In addition, they maintain leakage currents below 10 nA/mm across a wide voltage range from –650 V to +650 V. Although the inclusion of SSFPs introduces minimal parasitic resistance, resulting in a slight R_{ON} increase, the key advantage lies in their ability to substantially suppress current collapse, thereby enhancing long-term performance and reliability.

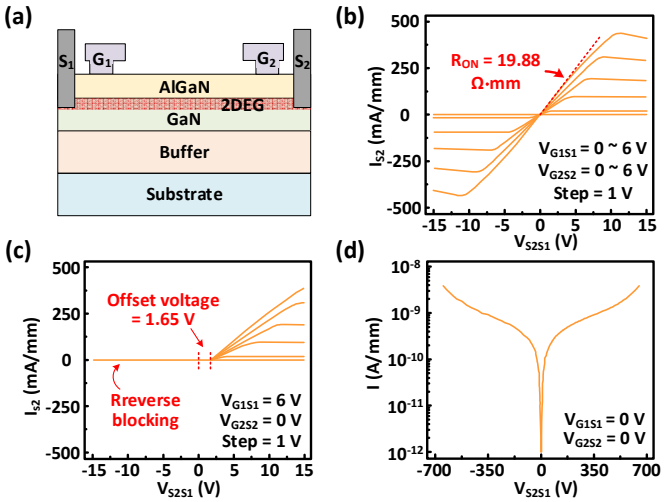

Fig. 6. The GFP MBD switch: (a) Simplified view, (b) Static I-V in bidirectional mode, (c) Static I-V in diode mode, (d) Static I-V in the off-state.

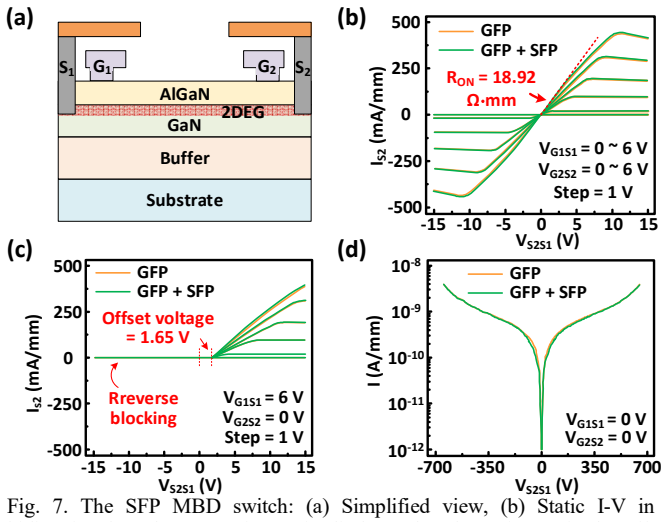

Fig. 7. The SFP MBD switch: (a) Simplified view, (b) Static I-V in bidirectional mode, (c) Static I-V in diode mode, (d) Static I-V in the off-state.

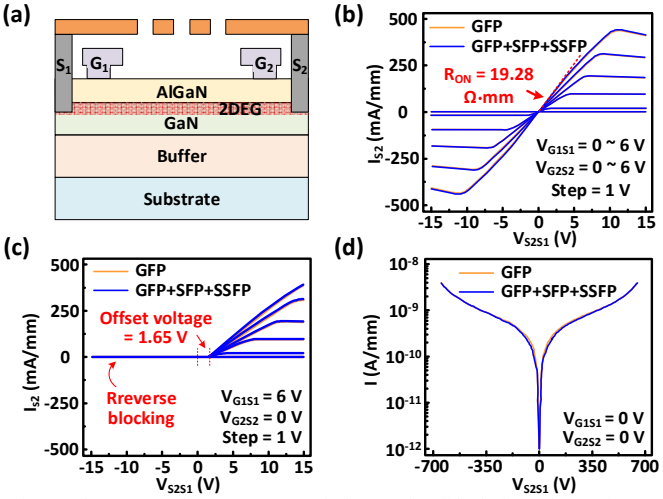

Fig. 8. The proposed SSFP MBD switch: (a) Simplified view, (b) Static I-V in bidirectional mode, (c) Static I-V in diode mode, (d) Static I-V in the off-state.

B. Pulse I-V characteristics

To assess the impact of current collapse on R_{ON}, pulse I-V measurements were performed using a 0.1 µs pulse width and a 0.1% duty cycle. Fig. 9 compares the pulse and static I-V characteristics of the three MBD switch configurations under stress conditions. The GFP MBD switch shows a significant rise in R_{ON} to 29.84 Ω·mm, representing a 50.1% rise from its static value, which indicates severe electron trapping. The SFP MBD switch reduces this effect, with R_{ON} increasing to 27.77 Ω·mm (a 46.7% rise), demonstrating partial mitigation. In contrast, the proposed SSFP MBD switch exhibits the most effective suppression, limiting R_{ON} to 24.91 Ω·mm under pulse conditions. These results confirm that integrating SFP and SSFP structures significantly alleviates current collapse, thereby minimizing conduction losses and improving overall efficiency.

Fig. 10 presents the wafer-level distributions of on-state resistance for GFP, SFP, and the proposed SSFP MBD switches, each based on 50 samples. Under static conditions, the SFP and SSFP configurations exhibit nearly identical R_{ON} values. However, under pulse conditions, the GFP configuration shows a ~50% increase in R_{ON}, indicating severe current collapse due to significant carrier trapping. The GFP + SFP configuration reduces this increase to ~46%, demonstrating partial suppression of trapping. Notably, the proposed GFP + SFP + SSFP configuration limits the R_{ON} increase to just 29%, confirming its superior effectiveness in mitigating trapping effects and minimizing current collapse.

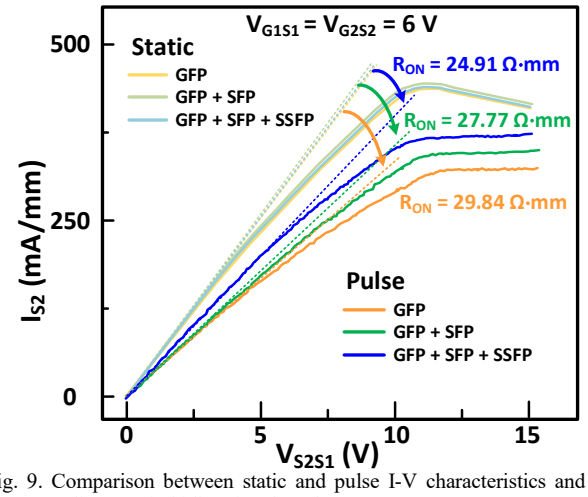

Fig. 9. Comparison between static and pulse I-V characteristics and their corresponding R_{ON} in bidirectional mode.

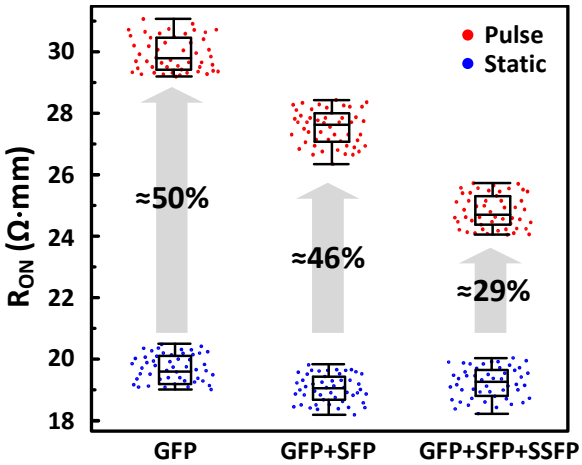

Fig. 10. Wafer distributions of R_{ON} for GFP, SFP, and the proposed SSFP MBD switches. Each group comprises 50 samples.

C. C-V characteristics

Fig. 11 illustrates the C–V characteristics of the GFP, SFP, and proposed SSFP MBD switches. The GFP MBD switch shows poor C_{rss} performance in (a) due to the lack of field plate structures. In contrast, the SFP and SSFP configurations introduce additional field plates, increasing overall parasitic capacitance. However, the SFP structure, through its series arrangement, helps suppress C_{rss}. The SSFP configuration further enhances this suppression by introducing a secondary C_{rss} step-down, typically observed around 100 V, indicating improved electric field modulation and reduced charge coupling.

The C_{oss} characteristics in Fig. 11(b) demonstrate the influence of SFP and SSFP structures across varying voltage ranges. The incorporation of SFPs induces multiple stepwise reductions in C_{oss} at lower voltages (below 100 V), while the added SSFPs effectively suppress the electric field at higher voltages (above 100 V), resulting in a significant overall reduction in C_{oss}. The ratio of C_{rss}/C_{iss} directly correlates with the Q_{GD}/Q_{GS} ratio, which significantly influences the device's immunity to gate voltage spikes and unintended switching events [10]. A lower C_{rss}/C_{iss} ratio enhances slew-rate immunity by minimizing gate voltage fluctuations

during transitions. Although the GFP MBD switch shows higher C_{iss} at low voltages (Fig. 11(c)), both the SFP and SSFP MBD switches offer better Miller ratio control. Notably, the proposed SSFP MBD switch further improves high-voltage performance by exhibiting a continued increase in C_{iss}, thereby optimizing switching behavior and stability.

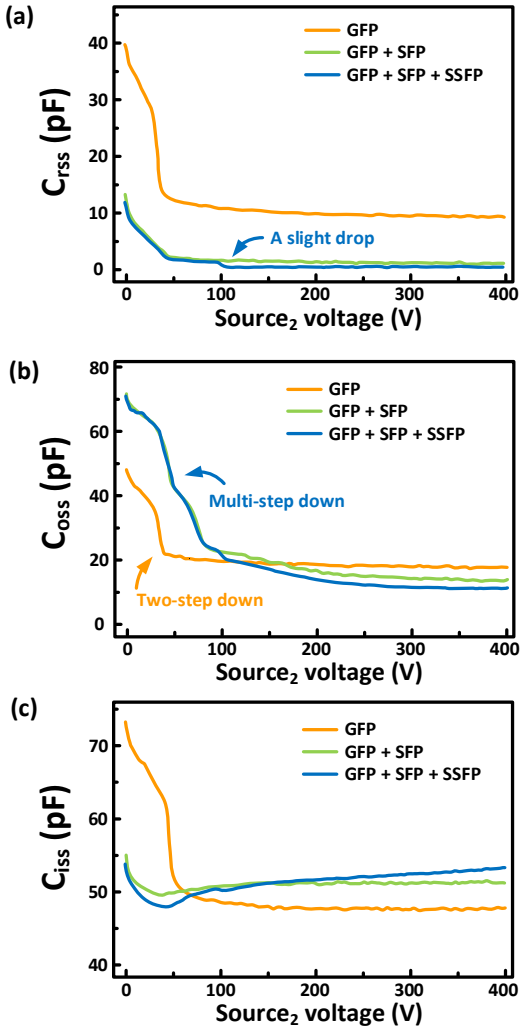

Fig. 11. Measured (a) C_{rss}, (b) C_{oss}, and (c) C_{iss} with three different field plate structures incorporated into MBD switches.

D. Chip Area

By sharing a common drain area, the proposed design significantly reduces the device cell pitch, resulting in a 31% area savings compared to conventional configurations using two discrete GaN HEMTs connected back-to-back, as illustrated in Fig. 12. This monolithic integration not only minimizes the overall chip footprint but also lowers parasitic inductance and resistance from interconnects, thereby improving electrical performance. Moreover, eliminating external bonding wires between discrete devices simplifies the packaging process and further reduces parasitic effects, contributing to enhanced overall efficiency.

V. Conclusion

This paper presents a Monolithic Bidirectional Dual-Gate (MBD) GaN HEMT switch architecture enhanced with Split Source Field Plates (SSFPs), delivering significant gains in performance and integration. The monolithic design reduces device area by 31% compared to traditional discrete back-to-back configurations while achieving lower R_{ON}. The addition of SSFPs effectively alleviates electric field crowding, substantially suppressing current collapse and ensuring R_{ON} stability under high-voltage off-state stress. Experimental results demonstrate a 42% reduction in R_{ON} degradation following repeated current collapse events. These improvements collectively boost the efficiency, reliability, and compactness of bidirectional GaN switches, positioning the proposed solution as a strong candidate for next-generation power electronics.

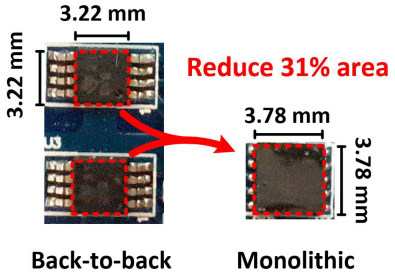

Fig. 12. Area comparison between back-to-back GaN switches and the proposed monolithic bidirectional dual-gate GaN switch.

Acknowledgment

The authors would like to thank Marvin Chang of Taiwan Semiconductor Manufacturing Company (TSMC) for his support in the JDP collaboration.

References

[1] R. Samanbakhsh, F. M. Ibanez, P. Koohi and F. Martin, "A New Asymmetric Cascaded Multilevel Converter Topology With Reduced Voltage Stress and Number of Switches," *IEEE Access*, vol. 9, pp. 92276-92287, 2021.

[2] P. W. Wheeler, J. Rodriguez, J. C. Clare, L. Empringham and A. Weinstein, "Matrix converters: a technology review," *IEEE Transactions on Industrial Electronics*, vol. 49, no. 2, pp. 276-288, April 2002.

[3] S. Dharmasena, T. O. Olowu and A. I. Sarwat, "Bidirectional AC/DC Converter Topologies: A Review," 2019 SoutheastCon, Huntsville, AL, USA, 2019, pp. 1-5.

[4] M. Y. Lee, P. Wheeler and C. Klumpner, "Space-Vector Modulated Multilevel Matrix Converter," *IEEE Transactions on Industrial Electronics*, vol. 57, no. 10, pp. 3385-3394, Oct. 2010.

[5] T. Morita et al., "650 V 3.1 mΩcm2 GaN-based monolithic bidirectional switch using normally-off gate injection transistor," *IEEE International Electron Devices Meeting*, Washington, DC, USA, pp. 865-868, 2007.

[6] S. Musumeci, M. Panizza, F. Stella and F. Perraud, "Monolithic Bidirectional Switch Based on GaN Gate Injection Transistors," 2020 *IEEE 29th International Symposium on Industrial Electronics (ISIE)*, Delft, Netherlands, pp. 1045-1050, 2020.

[7] G. Meneghesso, F. Rampazzo, P. Kordos, G. Verzellesi and E. Zanoni, "Current Collapse and High-Electric-Field Reliability of Unpassivated GaN/AlGaN/GaN HEMTs," *IEEE Transactions on Electron Devices*, vol. 53, no. 12, pp. 2932-2941, Dec. 2006.

[8] A. Brannick, N. A. Zakhleniuk, B. K. Ridley, J. R. Shealy, W. J. Schaff and L. F. Eastman, "Influence of Field Plate on the Transient Operation of the AlGaN/GaN HEMT," *IEEE Electron Device Letters*, vol. 30, no. 5, pp. 436-438, May 2009.

[9] W. Saito, Y. Kakiuchi, T. Nitta, Y. Saito, T. Noda, H. Fujimoto et al., "Field-Plate Structure Dependence of Current Collapse Phenomena in High-Voltage GaN-HEMTs," *IEEE Electron Device Letters*, vol. 31, no. 7, pp. 659-661, July 2010.

[10] P. Green, "Designing with power MOSFETs: How to avoid common issues and failure modes, Infineon Technologies," Application Note, 2019.